TYC 2402-0643-1: First Precision Photometric Observations and Analyses of the Totally Eclipsing, Solar Type Binary

Ronald G. Samec
Faculty Research Associate, Pisgah Astronomical Research Institute, 1 PARI Drive, Rosman, NC 28772; ronaldsamec@gmail.com

Daniel B. Caton
Dark Sky Observatory, Physics and Astronomy Department, Appalachian State University, 525 Rivers Street, Boone, NC 28608-2106; catondb@appstate.edu

Danny R. Faulkner
Johnson Observatory, 1414 Bur Oak Court, Hebron, KY 41048; dfaulkner@answersingenesis.org

Received March 28, 2020; revised April 22, May 11, 2020; accepted May 11, 2020

Abstract CCD BVRI light curves of TYC 2402-0643-1 were taken on 21, 22, and 23 January 2020 at the Dark Sky Observatory, Boone, North Carolina, with the 0.81-m reflector of Appalachian State by Daniel Caton. The variability of TYC 2402-0643-1 ([GGM2006] 6868894, NSVS 4382530) was discovered in the sky patrol data taken by the ROTSE-I telescope. It is classified as a contact variable with a maximum V magnitude of 11.373, an amplitude of V = 0.442, and a period of 0.399579 d. Three times of minimum light were determined from our present observations, which include one primary eclipse and two secondary eclipses. We selected three times of low light from ASAS observations and Gettel sent us some ROTSE data. From these we determined a 20-year study and a quadratic ephemeris. Thus, from our study, the period is found to be increasing. This could be due to mass transfer making the mass ratio ($q = M_2 / M_1$) decrease. A Wilson-Devinney analysis reveal that the system is an A-type W UMa binary (the hotter component is the more massive) with a somewhat extreme mass ratio, $q = 0.2079 \pm 0.0003$ (star 1 is the more massive, primary component, $1/q = M_1 / M_2 = 4.8$). Its Roche Lobe fill-out is ~22%. No spots were needed in the solution. The temperature difference of the components is only ~70 K, so it is in strong thermal contact. The inclination is high, $83.4 \pm 0.1°$, resulting in a total eclipse. As a result, the secondary minimum has a time of constant light with an eclipse duration of some 43 minutes.

1. Introduction

Many times, extreme mass ratio contact binaries (EMRBs, solar type, $q \lessapprox 0.2$, Samec *et al.* 2011) tend to become more extreme. In this case, the primary component is the gainer and the secondary component decreases in mass. In conservative mass exchange (Nelson and Alton 2019),

$$\frac{dM}{dt} = \frac{(dP/dt)\,(M_1\,M_2)}{[3P\,(M_1 - M_2)]} \quad . \qquad (1)$$

However, besides mass exchange, the mass is decaying from the system due to magnetic braking (Guinan and Bradstreet 1988). Magnetic braking happens in rotating solar type stars and binaries (Gharami *et al.* 2018). Solar type stars (roughly type FV to MV type stars) have deep convective envelopes made up of swirling plasmas that are magnetic in nature with strong dipole magnetic fields and magnetic phenomena, notably star spots (Mullen 1975; Vant'veer 1994). Stellar plasma winds escape from the North and South poles out to the Alfvén radius of the stars (about 15 solar radii). This allows the transport of mass particles on stiffly rotating magnetic field lines rotating with increasing radii, transferring angular momentum (L) into space (for a single particle, moving on radius, r, $L = mvr$) with expanding r. This continuously removes angular momentum, ΔL, from the binary causing angular momentum loss (AML, Loukaidou and Gazeas 2020). This effectively torques the star, $\tau = dL/dt$. For a single star, this causes the star's rotation to slow, finally resulting in a slow rotating star (from periods of a few days to about a month) like our present sun (Melendez *et al.* 2017; Guinan and Engle 2009). For a solar type binary system (two stars co-orbiting about a center of mass or barycenter), the same magnetic braking occurs but the orbital radius of the binary shrinks (Bradstreet and Guinan 1994) and by Kepler's third law, the orbital period shortens. When the atmospheres of the stars touch, the stars are called contact binaries. The stars continue to coalesce (Guinan *et al.* 1987) until they violently form, by a *red novae event* (Tylenda and Kamiński 2016; Molnar *et al.* 2017), fast-rotating single stars such as A-type stars, magnetic stars, or subgiants, similar to the spotted FK Comae stars in globular clusters (Schneider *et al.* 2019). An unpublished, extreme mass ratio binary, TYC 2402-0643-1, is reported on in this paper.

2. History and observations

The variability of TYC 2402-0643-1 ([GGM2006] 6868894, NSVS 4382530) was discovered in the sky patrol data taken by the ROTSE-I telescope (Gettel *et al.* 2006). They classified it as a contact variable with a maximum magnitude of $V_{max} = 11.373$, an amplitude of 0.442 V_{mag}, $J–K = 0.467$, and a period of 0.399579 d. ROTSE curves are shown in Figure 1. The binary appears in the automated variable star classification of variable stars (Hoffman *et al.* 2009) using the Northern Sky Variability Survey (NSVS; Hoffman *et al.* 2009). The system was also observed by the All

Sky Automated Survey as ASASSN-V J051858.09+365806.2 (Pojmański 2002). They give a $V_{mean} = 11.33$, an amplitude of 0.4, and EW designation, J–K = 0.467. Their ephemeris is:

$$\text{HJD Min I} = 2457070.80679 + 0.3995827\text{E d} \times \text{E} \qquad (2)$$

The ASAS curves are shown in Figure 2. From the ASAS and ROTSE curves we were able to phase the data with Equation 1 and the ROTSE period (0.399579 d) and construct parabola fits to the primary and secondary minima to locate several times of minimum light within 0.001 phase of each minimum.

This system was observed as a part of our professional collaborative studies of interacting binaries at Pisgah Astronomical Research Institute from data taken from DSO observations. The observations were taken by D. Caton, R. Samec, and D. Faulkner. Reduction and analyses were done by R. Samec.

Our BVRI light curves were taken at Dark Sky Observatory, on 21, 22, and 23 January 2020 with a thermoelectrically cooled (–35° C) 1K × 1K FLI camera and Bessel *BVRI* filters.

Individual observations included 264 images in Johnson-Cousins B, 282 in V, 311 in R_c, and 306 in I_c. The BVRI observations are given in Table 1. The probable error of a single observation was 4 mmag in B, V, and R, and 3 mmag in I. The nightly C–K values stayed constant throughout the observing run with a precision of about 1%. Exposure times varied from 45s in B, 20s in V, to 15s in R and I. To produce these results, nightly images were calibrated with 25 bias frames, at least five flat frames in each filter, and ten 300-second dark frames.

3. Photometric targets and finding chart

The photometric targets are given in Table 2. A finder chart of the field is given as Figure 3. The B, V, and B–V nightly light curves from 22 and 23 January 2020 are displayed in Figures 4 and 5.

4. Period study

Three mean times (from BVRI data) of minimum light were calculated and averaged from our present observations, one primary and two secondary eclipses:

$$\begin{aligned} \text{HJD I} &= 2457870.51294 \pm 0.00078, \\ \text{HJD II} &= 2457870.713587 \pm 0\ 0.00052, \\ &\ 2457871.512445 \pm 0.00078. \end{aligned}$$

These minima were weighted as 1.0 in the period study. In addition, four times of minimum light were calculated ASAS data and were weighted 0.1. Six other times of minimum light were taken from ROTSE data. These were not available publicly but were supplied by Dr. Sara Gettel (2020) at one author's request (Samec) and we wish to thank her for these data so that we were able to put together a reasonable period study.

From these timings, ephemerides have been calculated, a linear and a quadratic one:

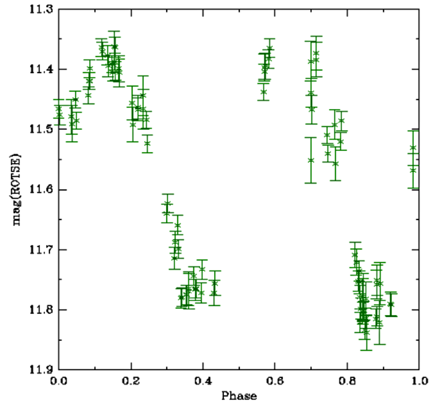

Figure 1. ROTSE light curves (Gettel *et al.* 2006).

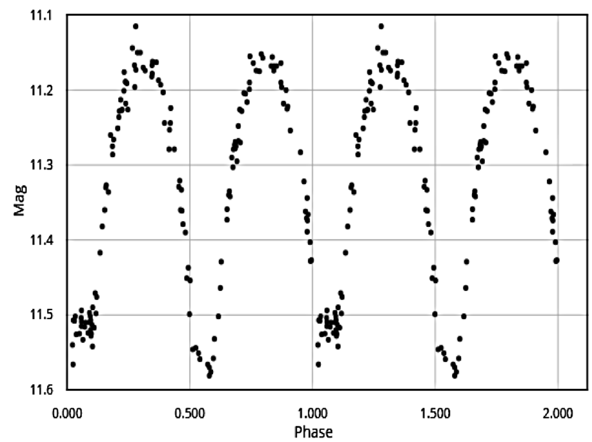

Figure 2. ASAS light curves (Pojmański 2002).

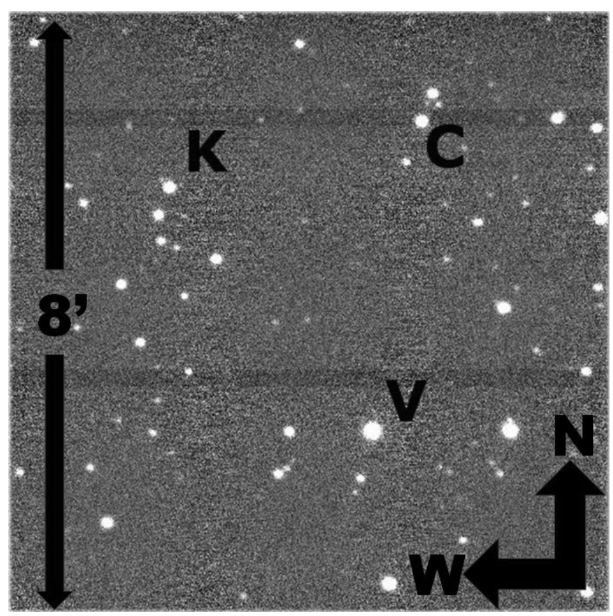

Figure 3. Finder chart: TYC 2402-0643-1 (V), comparison star (C), and check (K).

$$\text{JD Hel Min I} = 2458870.51289 \pm 0.00045\,\text{d} + 0.399578304 \pm 0.000000064 \times E \quad (3)$$

$$\text{JD Hel Min I} = 2458870.51346 \pm 0.00019\text{d} + 0.39958073 \pm 0.00000021 \times E + 0.000000000134 \pm 0.000000000012 \times E^2 \quad (4)$$

The study given here covers a time interval of ~20 years. It does show an orbital period that is increasing. If this effect is found to be correct, it might be due to mass transfer to the more massive, primary component making the mass ratio more extreme. The residuals are given in Table 3. The linear residuals are shown in Figure 6 and a plot of the quadratic term overlying the linear term residuals is given in Figure 7. The quadratic term B, V with B–V color curves and R, I curves with R–I color curves phased with Equation 3 are given in Figures 8 and 9, respectively.

The quadratic ephemeris yields a $\dot{P} = 8.77 \times 10^{-7}$ d / yr, or a mass exchange rate of

$$\frac{dM}{dt} = \frac{\dot{P} M_1 M_2}{3P\,(M_1 - M_2)} = \frac{-1.65\times10^{-8}\,M_\odot}{d}. \quad (5)$$

in a conservative scenario (the primary component is the gainer.)

5. Light curve characteristics

Averages of BVRI magnitudes from each quarter phase cycles, 0.0, 0.25, 0.50, and 0.75, are given in Table 4. From these, we can determine interesting characteristics of the curves. The curves are of good accuracy, averaging better than 1% photometric precision. The amplitude of the light curves varies from 0.35 to 0.47 mag. The O'Connell effect, a possible indicator of spot activity, averages less than the noise level. The differences in minima are small, 0.0–0.07 mag, indicating overcontact light curves in good thermal contact. A time of constant light occurs at our secondary minimum and lasts some 43 minutes.

6. Temperature and light curve solution

The 2MASS, J–K = 0.47 ± 0.02 for the binary star. These magnitudes correspond to ~K0V ± 2.5, which yields a temperature of 5250 ± 200 K. We use this temperature as the primary component's temperature in the light curve analysis. Fast rotating binary stars of this type are noted for having strong magnetic activity, so the binary is of solar type with a convective atmosphere.

7. Light curve solution

The B, V, R_c, and I_c curves were pre-modeled with BINARY MAKER 3.0 (Bradstreet and Steelman 2002). Fits were determined in all filter bands, which were very stable. The solution was that of an over contact eclipsing binary. The parameters were then averaged (q = 0.21, fill-out = 0.15, i = 80.25, T_2 = 5100, with one cool spot) and input into a four-color simultaneous

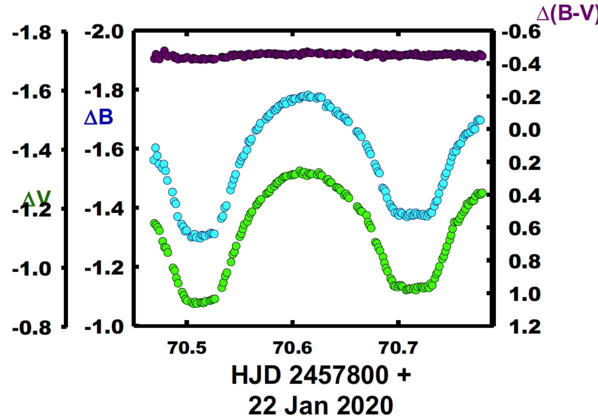

Figure. 4. TYC 2402-0643-1 B,V, B–V color curves from the evening of 22 January 2020.

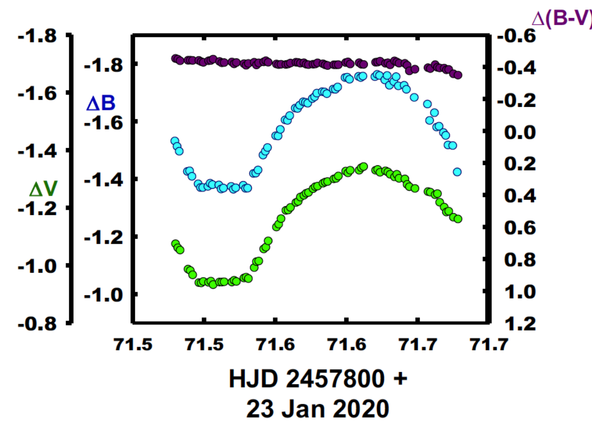

Figure. 5. TYC 2402-0643-1 B, V, B–V color curves from the evening of 23 January 2020.

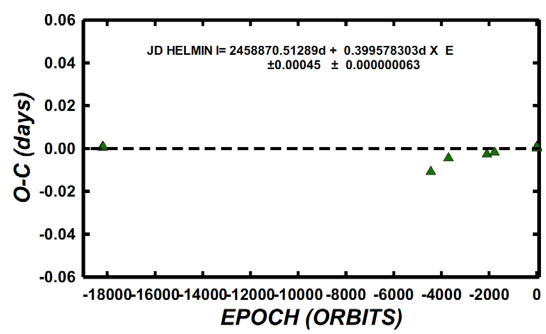

Figure 6. A plot of the linear residuals from Equation 3. The interval of the observations is some 20 years.

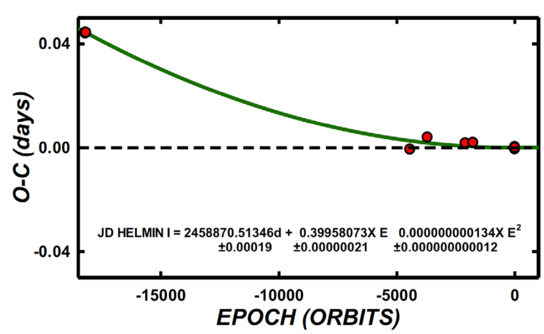

Figure 7. A plot of the quadratic term overlying the linear term residuals of Equation 4. The interval of the observations is some 20 years.

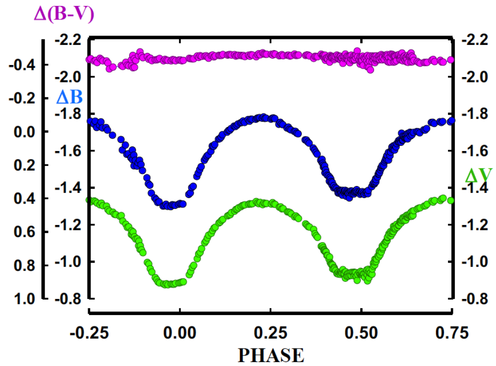

Figure 8. TYC 2402-0643-1 B,V plots and B–V color curves phased with Equation 1.

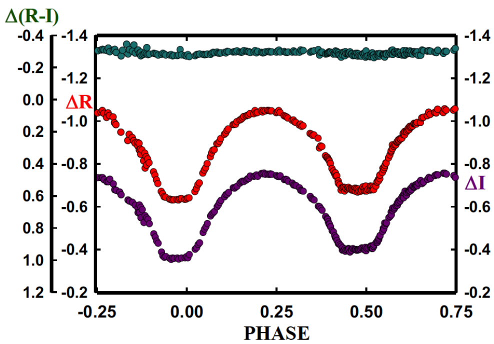

Figure 9. TYC 2402-0643-1 R, I plots and R–I color curves phased with Equation 1.

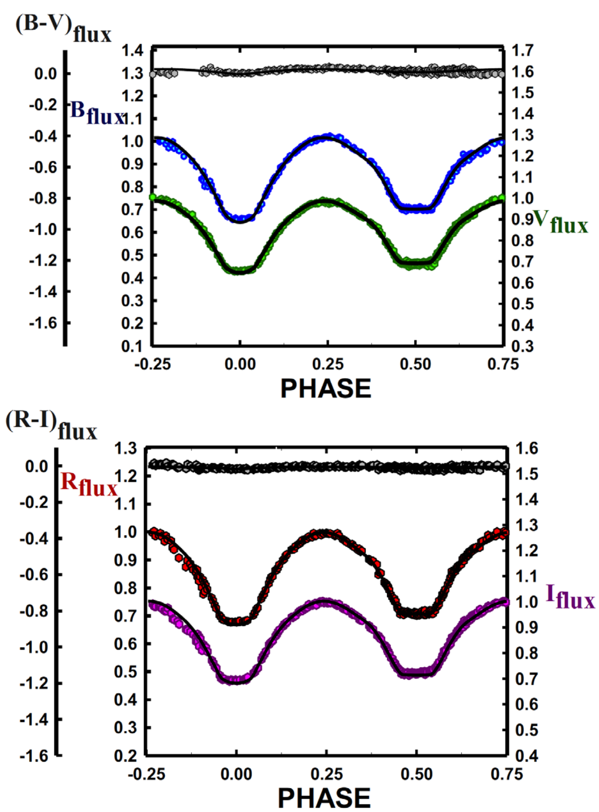

Figure 10. TYC 2402-0643-1: (a, upper plot) B, V normalized fluxes and the B–V color curves overlaid by the detached solution for TYC 2402-0643-1; (b, lower plot) R_c, I_c normalized fluxes and the R_c–I_c color curves overlaid by the over contact solution of TYC 2402-0643-1.

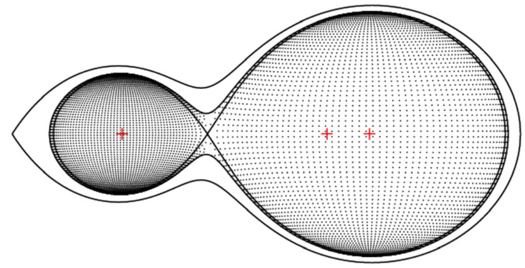

Figure 11. Solution of TYC 2402-0643-1 in cross-section showing the inner and outer Lagrangian surfaces and the fill-out (Bradstreet and Steelman 2002, BINARY BAKER 3.0).

light curve calculation using the Wilson-Devinney program (Wilson and Devinney 1971; Wilson 1979, 1990, 1994, 2008, 2012; Wilson *et al.* 2010; Van Hamme and Wilson 1998; Wilson and Van Hamme 2014). The solution was computed in Mode 3 and converged to a solution. Convective parameters g = 0.32, A = 0.5 (Lucy 1967; Ruciński 1969) were used.

An eclipse duration of ~43 minutes was determined for our secondary eclipse and the light curve solution. The more massive component is the hotter, making the system an A-type W UMa contact binary. We tried third light but that did not solve any fitting issues. The solution parameters follow in Table 5. The light curves of the BVRI solution with the solution curves overlay the mean flux values in Figures 10a and 10b. Figure 11 shows the geometric solution of TYC 2402-0643-1 in cross-section with the inner and outer Lagrangian surfaces and the fill-out.

TYC 2402-0643-1 is an A-type, W UMa binary. Since the eclipses were total, the mass ratio, q, is well determined (Terrell and Wilson 2005) with a fill-out of 22(1)%. The system has an extreme mass ratio of ~0.208, and a component temperature difference of only ~68 K, so it is in good thermal contact. No spots were needed in the final modeling. But there are various fluctuations about the smooth solution curve that indicate activity. Of the 25 EMRBs in Samec *et al.* (2011), three did not have modeled spots. However, for a solar-type binary such as this, that does not mean that there is no magnetic activity. Likely, the surface is saturated with magnetic activity, but is averaging out in flux level so the light curves are not a good means of detecting them. Doppler imaging of systems with fairly symmetric curves has shown many spots are actually present (Senavcı *et al.* 2011; Xiang *et al.* 2015). The inclination of ~83.4° resulted in a time of constant light in the secondary eclipse. Its photometric spectral type indicates a surface temperature of ~5250 K for the primary component, making it a solar type binary. Such a main sequence star would have a mass of ~0.86 $M_\odot$ and the secondary (from the mass ratio) would have a mass of ~0.18 $M_\odot$, making it very much undersized. The temperature (~5180 K) of a single main sequence star would make it of type K1V instead of M4.5V as indicated by its mass. At present the period study indicates that it is increasing. This could be due to mass exchange with the flow toward the primary, more massive component. Radial velocity curves are needed to obtain absolute (not relative) system parameters.

References

Bradstreet E. F., and Guinan, E. F. 1994, in *Interacting Binary Stars*, ed. A. W. Shafter, ASP Conf. Ser. 56, 228, Astronomical Society of the Pacific, San Francisco.

Bradstreet, D. H., and Steelman, D. P. 2002, *Bull. Amer. Astron. Soc.*, **34**, 1224.

Gaia Collaboration, Prusti, T., *et al.* 2016, *Astron. Astrophys.*, **595**, 1.

Gettel, S. J. 2020, Personal communication.

Gettel S. J., Geske M. T., and McKay T. A. 2006, *Astron. J.*, **131**, 621.

Gharami, P., Ghosh, K., and Rahaman, F. 2018, *Bull. Calcutta Math. Soc.*, **110**, 309.

Guinan, E. F., and Bradstreet, D. H. 1988, in *Formation and Evolution of Low Mass Stars*, eds. A. K. Dupree, M. T. V. T. Lago, NATO Adv. Sci. Inst. (ASI) Ser. C, 241, Kluwer, Dordrecht, 345.

Guinan, E. F., Bradstreet, D. H., and Robinson, C. R. 1987, *Bull. Amer. Astron. Soc.*, **19**, 1085.

Guinan, E. F., and Engle, E. G. 2009, in *The Ages of Stars*, eds. J. Th. van Loon, J. M. Oliveira, IAU Symp. 258, Cambridge Univ. Press, Cambridge, 395.

Hoffman, D. I., Harrison, T. E., and McNamara, B. J. 2009, *Astron. J.*, **138**, 466.

Loukaidou, G., and Gazeas, K. 2020, *Contrib. Astron. Obs. Skalnaté Pleso*, **50**, 461.

Lucy, L. B. 1967, *Z. Astrophys.*, **65**, 89.

Meléndez, J., dos Santos, L. A., and Freitas, F. C. 2017, in *Living Around Active Stars*, eds. D. Nandy, A. Valio, P. Petit, IAU Symp. 328, Cambridge Univ. Press, Cambridge, 274.

Molnar, L. A., *et al.* 2017, *Astrophys. J.*, **840**, 1.

Mullan, D. J. 1975, *Astrophys. J.*, **198**, 563.

Nelson, R. H., and Alton, K. B. 2019, *Inf. Bull. Var. Stars*, No. 6266, 1.

Ochsenbein, F., Bauer, P., and Marcout, J. 2000, *Astron. Astrophys., Suppl. Ser.*, **143**, 23.

Pojmański, G. 2002, *Acta. Astron.*, **52**, 397.

Ruciński, S. M. 1969, *Acta Astron.*, **19**, 245.

Samec, R. G., Labadorf, N. C., Hawkins, D. R., Faulkner, and Van Hamme, W. 2011, *Astron. J.*, **142**, 117.

Schneider, F. R., Ohlmann, S. T., Podsiadlowski, P., Röpke, F. K., Balbus, S. A., Pakmor, R., and Springel, V. 2019, *Nature*, **574**, 211.

Şenavcı, H. V., Hussain, G. A. J., O'Neal, D., and Barnes, J. 2011, *Astron. Astrophys.*, **529A**, 11.

Skrutskie, M. F., *et al.* 2006, *Astron. J.*, **131**, 1163.

Terrell D., and Wilson R. E. 2005, *Astrophys. Space Sci.*, **296**, 221.

Tylenda, R., and Kamiński, T. 2016, *Astron. Astrophys.*, **592A**, 134.

U.S. Naval Observatory. 2012, UCAC-3 (http://www.usno.navy.mil/USNO/astrometry/optical-IR-prod/ucac).

Van Hamme, W., and Wilson, R. E. 1998, Bull. Amer. Astron. Soc., 30, 1402.

Vant'veer, F. 1994, *Mem. Soc. Astron. Ital.*, **65**, 105.

Wilson, R. E. 1979, *Astrophys. J.*, **234**, 1054.

Wilson, R. E. 1990, *Astrophys. J.*, **356**, 613.

Wilson, R. E. 1994, *Publ. Astron. Soc. Pacific*, **106**, 921.

Wilson, R. E. 2008, *Astrophys. J.*, **672**, 575.

Wilson, R. E. 2012, *Astron. J.*, **144**, 73.

Wilson, R. E., and Devinney, E. J. 1971, *Astrophys. J.*, **166**, 605.

Wilson, R. E., and Van Hamme, W. 2014, *Astrophys. J.*, **780**, 151.

Wilson, R. E., Van Hamme, W., and Terrell, D. 2010, *Astrophys. J.*, **723**, 1469.

Xiang, Y., Gu, S., Collier Cameron, A., and Barnes, J. R. 2015, *Mon. Not. Roy. Astron. Soc.*, **447**, 567.

Table 1. TYC 2402-0643-1 observations, ΔB, ΔV, $ΔR_c$, and $ΔI_c$, variable star minus comparison star.

Δ*B*	*BHJD 2458800+*	Δ*B*	*BHJD 2458800+*	Δ*B*	*BHJD 2458800+*	Δ*B*	*BHJD 2458800+*	Δ*B*	*BHJD 2458800+*
–1.552	69.481	–1.322	70.500	–1.774	70.614	–1.377	70.724	–1.367	71.531
–1.509	69.483	–1.299	70.505	–1.781	70.615	–1.371	70.725	–1.418	71.535
–1.479	69.484	–1.302	70.506	–1.773	70.617	–1.370	70.728	–1.419	71.536
–1.479	69.486	–1.309	70.508	–1.774	70.618	–1.378	70.729	–1.430	71.538
–1.434	69.489	–1.298	70.509	–1.769	70.623	–1.384	70.731	–1.482	71.542
–1.446	69.491	–1.296	70.513	–1.774	70.625	–1.382	70.732	–1.495	71.543
–1.412	69.492	–1.306	70.515	–1.775	70.626	–1.404	70.734	–1.508	71.545
–1.398	69.494	–1.305	70.516	–1.772	70.628	–1.420	70.736	–1.549	71.550
–1.370	69.499	–1.303	70.518	–1.741	70.632	–1.423	70.737	–1.548	71.552
–1.386	69.500	–1.309	70.522	–1.752	70.634	–1.447	70.739	–1.571	71.554
–1.381	69.502	–1.313	70.523	–1.744	70.635	–1.472	70.742	–1.604	71.557
–1.358	69.503	–1.311	70.525	–1.739	70.637	–1.481	70.743	–1.602	71.559
–1.381	69.506	–1.310	70.526	–1.721	70.641	–1.506	70.744	–1.619	71.560
–1.368	69.509	–1.362	70.533	–1.726	70.643	–1.517	70.746	–1.645	71.564
–1.380	69.514	–1.370	70.535	–1.715	70.644	–1.538	70.748	–1.644	71.566
–1.364	69.516	–1.399	70.536	–1.711	70.645	–1.556	70.750	–1.655	71.567
–1.378	69.518	–1.406	70.538	–1.703	70.649	–1.573	70.751	–1.667	71.570
–1.388	69.519	–1.459	70.542	–1.703	70.650	–1.589	70.753	–1.665	71.571
–1.372	69.524	–1.477	70.543	–1.693	70.652	–1.591	70.755	–1.662	71.573
–1.362	69.527	–1.496	70.545	–1.690	70.653	–1.609	70.757	–1.678	71.576
–1.430	69.539	–1.512	70.547	–1.657	70.661	–1.614	70.758	–1.684	71.578
–1.442	69.540	–1.547	70.550	–1.656	70.663	–1.617	70.759	–1.697	71.579
–1.456	69.542	–1.559	70.551	–1.646	70.664	–1.637	70.762	–1.702	71.583
–1.473	69.544	–1.570	70.553	–1.639	70.665	–1.646	70.763	–1.701	71.585
–1.519	69.547	–1.576	70.554	–1.613	70.670	–1.650	70.765	–1.695	71.586
–1.518	69.549	–1.595	70.557	–1.602	70.671	–1.651	70.766	–1.711	71.591
–1.547	69.551	–1.624	70.559	–1.590	70.673	–1.656	70.769	–1.710	71.592
–1.570	69.552	–1.622	70.560	–1.580	70.674	–1.674	70.770	–1.718	71.594
–1.592	69.556	–1.632	70.562	–1.547	70.678	–1.665	70.771	–1.751	71.599
–1.619	69.558	–1.661	70.566	–1.535	70.680	–1.665	70.773	–1.752	71.601
–1.625	69.560	–1.664	70.567	–1.521	70.681	–1.693	70.775	–1.745	71.602
–1.626	69.561	–1.672	70.569	–1.516	70.683	–1.698	70.777	–1.755	71.609
–1.653	69.565	–1.685	70.570	–1.466	70.685	–1.695	70.778	–1.751	71.610
–1.658	69.567	–1.699	70.575	–1.462	70.687	–1.531	71.480	–1.756	71.612
–1.693	69.569	–1.708	70.577	–1.454	70.688	–1.512	71.481	–1.754	71.620
–1.677	69.570	–1.709	70.578	–1.432	70.690	–1.495	71.483	–1.762	71.622
–1.681	69.573	–1.718	70.580	–1.410	70.693	–1.425	71.488	–1.758	71.623
–1.691	69.575	–1.731	70.583	–1.400	70.694	–1.427	71.490	–1.743	71.627
–1.560	70.469	–1.729	70.584	–1.395	70.696	–1.408	71.492	–1.758	71.629
–1.602	70.471	–1.735	70.586	–1.382	70.697	–1.382	71.496	–1.724	71.630
–1.575	70.472	–1.743	70.587	–1.381	70.700	–1.369	71.498	–1.737	71.633
–1.547	70.474	–1.749	70.590	–1.372	70.701	–1.369	71.499	–1.754	71.635
–1.533	70.477	–1.751	70.591	–1.384	70.702	–1.373	71.503	–1.722	71.637
–1.547	70.479	–1.759	70.593	–1.380	70.704	–1.384	71.504	–1.724	71.641
–1.524	70.480	–1.751	70.594	–1.372	70.707	–1.379	71.506	–1.710	71.642
–1.491	70.482	–1.767	70.598	–1.374	70.710	–1.378	71.511	–1.682	71.648
–1.452	70.487	–1.758	70.600	–1.381	70.712	–1.364	71.512	–1.659	71.657
–1.420	70.488	–1.768	70.601	–1.372	70.714	–1.367	71.514	–1.629	71.662
–1.412	70.490	–1.768	70.603	–1.374	70.715	–1.373	71.519	–1.560	71.668
–1.369	70.492	–1.768	70.607	–1.382	70.717	–1.363	71.521	–1.550	71.670
–1.343	70.495	–1.774	70.608	–1.376	70.718	–1.368	71.522	–1.517	71.671
–1.334	70.497	–1.776	70.610	–1.376	70.721	–1.377	71.528	–1.515	71.675
–1.319	70.499	–1.777	70.611	–1.372	70.723	–1.366	71.529		

Table continued on following pages

Table 1. TYC 2402-0643-1 observations, ΔB, ΔV, $ΔR_c$, and $ΔI_c$, variable star minus comparison star, cont.

ΔV	VHJD 2458800+	ΔV	VHJD 2458800+	ΔV	VHJD 2458800+	ΔV	VHJD 2458800+	ΔV	VHJD 2458800+
–1.085	69.481	–0.943	70.492	–1.307	70.614	–0.942	70.731	–1.132	71.551
–1.059	69.483	–0.913	70.496	–1.316	70.616	–0.936	70.733	–1.142	71.553
–1.054	69.485	–0.902	70.498	–1.312	70.617	–0.959	70.735	–1.161	71.554
–1.033	69.486	–0.889	70.499	–1.313	70.619	–0.974	70.736	–1.190	71.558
–1.024	69.489	–0.884	70.501	–1.310	70.624	–0.981	70.738	–1.191	71.559
–0.988	69.491	–0.878	70.505	–1.318	70.625	–1.000	70.739	–1.200	71.561
–0.960	69.493	–0.874	70.507	–1.310	70.627	–1.025	70.742	–1.217	71.565
–0.967	69.494	–0.880	70.508	–1.308	70.628	–1.035	70.743	–1.221	71.566
–0.942	69.499	–0.874	70.510	–1.293	70.633	–1.051	70.745	–1.236	71.568
–0.936	69.501	–0.878	70.514	–1.295	70.634	–1.068	70.746	–1.242	71.570
–0.937	69.502	–0.877	70.515	–1.284	70.636	–1.089	70.749	–1.249	71.572
–0.956	69.504	–0.877	70.517	–1.285	70.637	–1.106	70.750	–1.252	71.573
–0.910	69.507	–0.882	70.518	–1.268	70.642	–1.128	70.752	–1.265	71.577
–0.921	69.508	–0.884	70.522	–1.267	70.643	–1.150	70.753	–1.272	71.578
–0.936	69.510	–0.886	70.524	–1.264	70.644	–1.152	70.756	–1.274	71.580
–0.938	69.512	–0.889	70.525	–1.257	70.646	–1.151	70.757	–1.284	71.584
–0.938	69.515	–0.890	70.527	–1.241	70.649	–1.162	70.758	–1.288	71.585
–0.939	69.516	–0.928	70.533	–1.246	70.651	–1.174	70.760	–1.290	71.587
–0.940	69.518	–0.945	70.535	–1.238	70.652	–1.185	70.762	–1.299	71.591
–0.935	69.523	–0.968	70.537	–1.232	70.654	–1.194	70.764	–1.301	71.593
–0.936	69.525	–0.979	70.538	–1.203	70.662	–1.212	70.765	–1.309	71.594
–0.933	69.526	–1.015	70.542	–1.196	70.663	–1.208	70.767	–1.326	71.600
–0.915	69.528	–1.041	70.544	–1.188	70.664	–1.222	70.769	–1.320	71.601
–0.912	69.533	–1.049	70.545	–1.186	70.666	–1.221	70.770	–1.329	71.603
–0.937	69.534	–1.069	70.547	–1.173	70.670	–1.223	70.772	–1.329	71.609
–0.931	69.536	–1.101	70.550	–1.150	70.672	–1.238	70.773	–1.338	71.611
–0.997	69.539	–1.111	70.552	–1.130	70.675	–1.248	70.776	–1.342	71.612
–1.013	69.541	–1.127	70.553	–1.082	70.679	–1.243	70.777	–1.329	71.621
–1.030	69.542	–1.142	70.555	–1.078	70.680	–1.244	70.778	–1.332	71.622
–1.052	69.544	–1.152	70.558	–1.064	70.682	–1.249	70.780	–1.322	71.624
–1.076	69.548	–1.167	70.559	–1.053	70.683	–1.074	71.480	–1.327	71.628
–1.096	69.549	–1.180	70.561	–1.032	70.686	–1.060	71.482	–1.323	71.629
–1.107	69.551	–1.185	70.562	–1.012	70.687	–1.052	71.483	–1.315	71.631
–1.114	69.553	–1.208	70.566	–0.994	70.689	–0.986	71.489	–1.306	71.634
–1.138	69.557	–1.213	70.568	–0.983	70.690	–0.981	71.491	–1.315	71.635
–1.162	69.558	–1.222	70.569	–0.959	70.693	–0.966	71.492	–1.301	71.637
–1.178	69.560	–1.227	70.570	–0.951	70.695	–0.939	71.497	–1.299	71.641
–1.180	69.562	–1.246	70.576	–0.935	70.696	–0.938	71.498	–1.280	71.643
–1.196	69.566	–1.250	70.577	–0.932	70.697	–0.943	71.500	–1.272	71.644
–1.214	69.567	–1.253	70.579	–0.930	70.700	–0.940	71.503	–1.266	71.648
–1.220	69.569	–1.264	70.580	–0.936	70.701	–0.944	71.505	–1.255	71.650
–1.231	69.571	–1.272	70.583	–0.936	70.703	–0.932	71.507	–1.253	71.651
–1.242	69.574	–1.281	70.585	–0.932	70.704	–0.941	71.511	–1.244	71.656
–1.240	69.576	–1.283	70.586	–0.920	70.708	–0.941	71.513	–1.248	71.657
–1.253	69.577	–1.290	70.588	–0.921	70.709	–0.942	71.514	–1.218	71.659
–1.246	69.579	–1.296	70.590	–0.925	70.711	–0.941	71.520	–1.201	71.662
–1.146	70.470	–1.302	70.592	–0.924	70.712	–0.947	71.521	–1.184	71.664
–1.140	70.471	–1.304	70.593	–0.923	70.715	–0.943	71.523	–1.187	71.666
–1.132	70.473	–1.306	70.595	–0.928	70.716	–0.955	71.528	–1.166	71.669
–1.121	70.475	–1.309	70.599	–0.920	70.717	–0.958	71.530	–1.160	71.670
–1.085	70.478	–1.312	70.600	–0.930	70.719	–0.953	71.531	–1.134	71.672
–1.065	70.479	–1.310	70.602	–0.931	70.722	–0.991	71.535	–1.122	71.675
–1.063	70.481	–1.312	70.603	–0.931	70.723	–1.012	71.537	–1.110	71.677
–1.047	70.482	–1.324	70.607	–0.926	70.724	–1.014	71.539	–1.085	71.678
–0.995	70.487	–1.316	70.609	–0.931	70.726	–1.056	71.542		
–0.986	70.489	–1.312	70.610	–0.934	70.728	–1.062	71.544		
–0.961	70.491	–1.319	70.612	–0.927	70.730	–1.084	71.545		

Table continued on following pages

Table 1. TYC 2402-0643-1 observations, ΔB, ΔV, ΔR_c, and ΔI_c, variable star minus comparison star, cont.

Δ*R*	*RHJD 2458800+*	Δ*R*	*RHJD 2458800+*	Δ*R*	*RHJD 2458800+*	Δ*R*	*RHJD 2458800+*	Δ*R*	*RHJD 2458800+*
–0.829	71.479	–1.018	71.640	–0.983	70.576	–0.677	70.707	–0.694	71.528
–0.817	71.480	–0.991	71.641	–0.984	70.577	–0.675	70.708	–0.688	71.530
–0.801	71.482	–0.982	71.643	–0.996	70.579	–0.675	70.709	–0.714	71.534
–0.757	71.488	–0.947	71.648	–1.004	70.582	–0.671	70.711	–0.726	71.536
–0.743	71.489	–0.908	71.656	–1.007	70.584	–0.667	70.713	–0.746	71.537
–0.719	71.491	–0.937	71.658	–1.013	70.585	–0.672	70.715	–0.779	71.541
–0.687	71.495	–0.922	71.661	–1.020	70.586	–0.670	70.716	–0.782	71.542
–0.689	71.497	–0.907	71.663	–1.023	70.589	–0.675	70.718	–0.803	71.544
–0.688	71.498	–0.896	71.664	–1.026	70.591	–0.675	70.720	–0.855	71.550
–0.687	71.502	–0.882	71.667	–1.027	70.592	–0.672	70.722	–0.870	71.551
–0.683	71.504	–0.864	71.669	–1.034	70.594	–0.672	70.723	–0.881	71.553
–0.682	71.505	–0.844	71.671	–1.033	70.598	–0.679	70.725	–0.900	71.556
–0.685	71.510	–0.813	71.674	–1.048	70.599	–0.676	70.727	–0.911	71.558
–0.683	71.511	–0.793	71.677	–1.037	70.600	–0.679	70.728	–0.916	71.560
–0.681	71.513	–0.899	70.468	–1.039	70.602	–0.678	70.730	–0.942	71.563
–0.691	71.518	–0.895	70.470	–1.048	70.606	–0.678	70.731	–0.950	71.565
–0.685	71.520	–0.868	70.472	–1.041	70.608	–0.695	70.734	–0.953	71.567
–0.695	71.522	–0.864	70.473	–1.048	70.609	–0.714	70.735	–0.966	71.569
–0.695	71.527	–0.849	70.476	–1.046	70.610	–0.719	70.737	–0.974	71.571
–0.694	71.528	–0.833	70.478	–1.049	70.613	–0.729	70.738	–0.972	71.572
–0.688	71.530	–0.822	70.480	–1.048	70.615	–0.759	70.741	–0.988	71.575
–0.714	71.534	–0.804	70.481	–1.046	70.616	–0.772	70.742	–0.987	71.577
–0.726	71.536	–0.762	70.486	–1.047	70.617	–0.792	70.744	–0.992	71.579
–0.746	71.537	–0.746	70.488	–1.038	70.623	–0.803	70.745	–0.992	71.582
–0.779	71.541	–0.724	70.489	–1.041	70.624	–0.827	70.748	–1.014	71.584
–0.782	71.542	–0.707	70.491	–1.048	70.626	–0.840	70.749	–1.016	71.586
–0.803	71.544	–0.670	70.495	–1.039	70.627	–0.860	70.751	–1.024	71.590
–0.855	71.550	–0.659	70.496	–1.024	70.631	–0.888	70.752	–1.040	71.592
–0.870	71.551	–0.645	70.498	–1.021	70.633	–0.888	70.754	–1.030	71.593
–0.881	71.553	–0.643	70.499	–1.018	70.634	–0.888	70.756	–1.039	71.598
–0.900	71.556	–0.634	70.504	–1.013	70.636	–0.903	70.757	–1.037	71.600
–0.911	71.558	–0.632	70.505	–1.003	70.640	–0.905	70.759	–1.054	71.601
–0.916	71.560	–0.630	70.507	–1.004	70.642	–0.915	70.761	–1.039	71.608
–0.942	71.563	–0.631	70.509	–0.995	70.643	–0.919	70.763	–1.056	71.609
–0.950	71.565	–0.632	70.512	–0.992	70.645	–0.936	70.764	–1.050	71.611
–0.953	71.567	–0.630	70.514	–0.980	70.648	–0.934	70.766	–1.050	71.619
–0.966	71.569	–0.635	70.515	–0.985	70.650	–0.949	70.768	–1.056	71.621
–0.974	71.571	–0.637	70.517	–0.974	70.651	–0.956	70.769	–1.037	71.622
–0.972	71.572	–0.633	70.521	–0.977	70.653	–0.959	70.771	–1.041	71.626
–0.988	71.575	–0.634	70.522	–0.941	70.660	–0.968	70.772	–1.048	71.628
–0.987	71.577	–0.639	70.524	–0.938	70.662	–0.975	70.774	–1.035	71.629
–0.992	71.579	–0.640	70.526	–0.932	70.663	–0.986	70.776	–1.016	71.633
–0.992	71.582	–0.669	70.532	–0.934	70.665	–0.986	70.777	–1.037	71.634
–1.014	71.584	–0.683	70.534	–0.919	70.669	–0.985	70.779	–1.025	71.636
–1.016	71.586	–0.701	70.535	–0.873	70.671	–0.829	71.479	–1.018	71.640
–1.024	71.590	–0.710	70.537	–0.883	70.672	–0.817	71.480	–0.991	71.641
–1.040	71.592	–0.756	70.541	–0.880	70.674	–0.801	71.482	–0.982	71.643
–1.030	71.593	–0.770	70.543	–0.837	70.678	–0.757	71.488	–0.947	71.648
–1.039	71.598	–0.781	70.544	–0.829	70.679	–0.743	71.489	–0.908	71.656
–1.037	71.600	–0.800	70.546	–0.822	70.680	–0.719	71.491	–0.937	71.658
–1.054	71.601	–0.832	70.549	–0.812	70.682	–0.687	71.495	–0.922	71.661
–1.039	71.608	–0.850	70.551	–0.777	70.685	–0.689	71.497	–0.907	71.663
–1.056	71.609	–0.863	70.552	–0.765	70.686	–0.688	71.498	–0.896	71.664
–1.050	71.611	–0.865	70.554	–0.753	70.688	–0.687	71.502	–0.882	71.667
–1.050	71.619	–0.893	70.557	–0.741	70.689	–0.683	71.504	–0.864	71.669
–1.056	71.621	–0.894	70.558	–0.708	70.692	–0.682	71.505	–0.844	71.671
–1.037	71.622	–0.904	70.559	–0.701	70.693	–0.685	71.510	–0.813	71.674
–1.041	71.626	–0.917	70.561	–0.676	70.695	–0.683	71.511	–0.779	71.675
–1.048	71.628	–0.937	70.565	–0.686	70.696	–0.681	71.513	–0.793	71.677
–1.035	71.629	–0.943	70.566	–0.672	70.699	–0.691	71.518		
–1.016	71.633	–0.955	70.568	–0.682	70.700	–0.685	71.520		
–1.037	71.634	–0.962	70.569	–0.682	70.702	–0.695	71.522		
–1.025	71.636	–0.982	70.575	–0.689	70.703	–0.695	71.527		

Table continued onnext page

Table 1. TYC 2402-0643-1 observations, ΔB, ΔV, $ΔR_c$, and $ΔI_c$, variable star minus comparison star, cont.

ΔI	IHJD 2458800+	ΔI	IHJD 2458800+	ΔI	IHJD 2458800+	ΔI	IHJD 2458800+	ΔI	IHJD 2458800+
–0.540	71.479	–0.727	71.636	–0.694	70.579	–0.403	70.708	–0.415	71.527
–0.518	71.481	–0.705	71.640	–0.709	70.582	–0.399	70.710	–0.403	71.529
–0.505	71.482	–0.678	71.642	–0.715	70.584	–0.398	70.711	–0.413	71.530
–0.453	71.488	–0.675	71.643	–0.718	70.585	–0.398	70.714	–0.432	71.534
–0.441	71.490	–0.667	71.647	–0.716	70.587	–0.398	70.715	–0.445	71.536
–0.426	71.491	–0.654	71.649	–0.723	70.589	–0.401	70.716	–0.464	71.538
–0.396	71.496	–0.630	71.656	–0.729	70.591	–0.406	70.718	–0.497	71.541
–0.396	71.497	–0.625	71.658	–0.730	70.592	–0.400	70.721	–0.522	71.543
–0.391	71.499	–0.619	71.661	–0.742	70.594	–0.409	70.722	–0.520	71.544
–0.403	71.502	–0.606	71.665	–0.740	70.598	–0.404	70.724	–0.574	71.550
–0.387	71.504	–0.571	71.668	–0.742	70.599	–0.407	70.725	–0.592	71.552
–0.398	71.506	–0.572	71.669	–0.747	70.601	–0.411	70.727	–0.588	71.553
–0.399	71.510	–0.592	70.469	–0.740	70.602	–0.412	70.729	–0.605	71.557
–0.395	71.512	–0.607	70.470	–0.754	70.606	–0.404	70.730	–0.619	71.558
–0.397	71.513	–0.596	70.472	–0.752	70.608	–0.420	70.732	–0.625	71.560
–0.405	71.519	–0.585	70.474	–0.756	70.609	–0.431	70.734	–0.640	71.564
–0.397	71.520	–0.557	70.477	–0.750	70.611	–0.440	70.735	–0.671	71.565
–0.393	71.522	–0.547	70.478	–0.751	70.613	–0.452	70.737	–0.652	71.567
–0.415	71.527	–0.540	70.480	–0.749	70.615	–0.461	70.738	–0.668	71.569
–0.403	71.529	–0.519	70.481	–0.752	70.616	–0.483	70.741	–0.672	71.571
–0.413	71.530	–0.472	70.486	–0.750	70.618	–0.494	70.743	–0.678	71.572
–0.432	71.534	–0.457	70.488	–0.744	70.623	–0.511	70.744	–0.692	71.576
–0.445	71.536	–0.438	70.490	–0.740	70.624	–0.523	70.745	–0.701	71.577
–0.464	71.538	–0.428	70.491	–0.739	70.626	–0.547	70.748	–0.696	71.579
–0.497	71.541	–0.387	70.495	–0.743	70.627	–0.553	70.749	–0.721	71.583
–0.522	71.543	–0.369	70.497	–0.725	70.632	–0.560	70.751	–0.707	71.584
–0.520	71.544	–0.362	70.498	–0.727	70.633	–0.580	70.752	–0.713	71.586
–0.574	71.550	–0.366	70.500	–0.725	70.635	–0.594	70.755	–0.726	71.590
–0.592	71.552	–0.357	70.504	–0.717	70.636	–0.603	70.756	–0.735	71.592
–0.588	71.553	–0.352	70.506	–0.709	70.641	–0.616	70.758	–0.730	71.593
–0.605	71.557	–0.359	70.507	–0.700	70.642	–0.626	70.759	–0.744	71.599
–0.619	71.558	–0.357	70.509	–0.699	70.643	–0.636	70.762	–0.748	71.600
–0.625	71.560	–0.359	70.513	–0.697	70.645	–0.646	70.763	–0.747	71.602
–0.640	71.564	–0.354	70.514	–0.687	70.649	–0.655	70.764	–0.755	71.608
–0.671	71.565	–0.359	70.517	–0.675	70.650	–0.661	70.766	–0.755	71.610
–0.652	71.567	–0.360	70.521	–0.673	70.651	–0.665	70.768	–0.751	71.611
–0.668	71.569	–0.365	70.523	–0.671	70.653	–0.672	70.769	–0.744	71.620
–0.672	71.571	–0.360	70.524	–0.647	70.661	–0.673	70.771	–0.735	71.621
–0.678	71.572	–0.375	70.526	–0.637	70.662	–0.684	70.772	–0.734	71.623
–0.692	71.576	–0.400	70.532	–0.633	70.664	–0.695	70.775	–0.734	71.627
–0.701	71.577	–0.407	70.534	–0.630	70.665	–0.688	70.776	–0.734	71.628
–0.696	71.579	–0.422	70.536	–0.601	70.670	–0.696	70.778	–0.725	71.630
–0.721	71.583	–0.430	70.537	–0.599	70.671	–0.702	70.779	–0.715	71.633
–0.707	71.584	–0.478	70.541	–0.590	70.672	–0.709	70.781	–0.715	71.634
–0.713	71.586	–0.494	70.543	–0.582	70.674	–0.540	71.479	–0.727	71.636
–0.726	71.590	–0.505	70.544	–0.553	70.678	–0.518	71.481	–0.705	71.640
–0.735	71.592	–0.520	70.546	–0.544	70.679	–0.505	71.482	–0.678	71.642
–0.730	71.593	–0.555	70.550	–0.528	70.681	–0.453	71.488	–0.675	71.643
–0.744	71.599	–0.564	70.551	–0.517	70.682	–0.441	71.490	–0.667	71.647
–0.748	71.600	–0.570	70.552	–0.486	70.685	–0.426	71.491	–0.654	71.649
–0.747	71.602	–0.576	70.554	–0.481	70.686	–0.396	71.496	–0.630	71.656
–0.755	71.608	–0.598	70.557	–0.463	70.688	–0.396	71.497	–0.625	71.658
–0.755	71.610	–0.607	70.558	–0.456	70.689	–0.391	71.499	–0.619	71.661
–0.751	71.611	–0.619	70.560	–0.429	70.692	–0.403	71.502	–0.606	71.665
–0.744	71.620	–0.628	70.561	–0.421	70.694	–0.387	71.504	–0.571	71.668
–0.735	71.621	–0.645	70.565	–0.415	70.695	–0.398	71.506	–0.572	71.669
–0.734	71.623	–0.655	70.567	–0.407	70.697	–0.399	71.510	–0.547	71.671
–0.734	71.627	–0.657	70.568	–0.402	70.699	–0.395	71.512	–0.525	71.674
–0.734	71.628	–0.665	70.570	–0.397	70.701	–0.397	71.513		
–0.725	71.630	–0.687	70.575	–0.398	70.702	–0.405	71.519		
–0.715	71.633	–0.685	70.576	–0.400	70.703	–0.397	71.520		
–0.715	71.634	–0.690	70.578	–0.394	70.707	–0.393	71.522		

Table 2. Information on the stars used in this study.

Star	*Name*	*R.A. (2000)* h m s	*Dec. (2000)*[1] ° ′ ″	*V*	*J–K*
V (Variable)	TYC 2402-0643-1 GSC 4547 0771 2MASS J05185809+3658060 ASAS J113031-0101.9 NSVS 4382530 [GGM2006] 6868894	05 18 58.0949883180	+36 58 06.076375043[1]	11.373[2]	0.467 ± 0.049[2]
C (Comparison)	GSC 2402 0273 3UC255-052567[3]	05 19 01.8633	+37 02 53.47[2]	12.07[3]	0.68[4]
K (Check)	GSC 2402 1209 3UC255-052413[3]	05 18 41.3125	+37 01 51.489[2]	12.36[2]	0.420 ± 0.046[2]

[1] *Gaia Collaboration (2006).* [2] *VizieR (Ochsenbein* et al. *2000).* [3] *UCAC3 (U.S. Naval Obs. 2012).* [4] *2MASS (Skrutskie* et al. *2006).*

Table 3. O–C Residuals for TYC 2402 0643 1.

	Epochs	*Cycles*	*Linear Residuals*	*Quadratic Residuals*	*Weight*	*Error*	*References*
1	51597.1893	–18202.5	0.0005	–0.0002	0.1	0.0007	Gettel et al. (2006) (ROTSE)
2	51597.1896	–18202.5	0.0008	0.0001	0.1	0.0001	Gettel et al. (2006) (ROTSE)
3	51607.1791	–18177.5	0.0008	0.0002	0.1	0.0001	Gettel et al. (2006) (ROTSE)
4	51597.3891	–18202.0	0.0005	–0.0002	0.1	0.0006	Gettel et al. (2006) (ROTSE)
5	51597.3894	–18202.0	0.0008	0.0001	0.1	0.0002	Gettel et al. (2006) (ROTSE)
6	51607.3789	–18177.0	0.0008	0.0002	0.1	0.0002	Gettel et al. (2006) (ROTSE)
7	57095.7750	–4441.5	–0.0109	–0.0033	0.1	0.0003	Pojmański (2002)
8	57390.8700	–3703.0	–0.0044	0.0021	0.1	0.0115	Pojmański (2002)
9	58033.9930	–2093.5	–0.0027	0.0012	0.1	0.0063	Pojmański (2002)
10	58161.8590	–1773.5	–0.0018	0.0015	0.1	0.0066	Pojmański (2002)
11	58870.5129	0.0	0.0000	–0.0005	1.0	0.0004	Present observations
12	58870.7136	0.5	0.0009	0.0003	1.0	0.0005	Present observations
13	58871.5125	2.5	0.0006	0.0000	1.0	0.0008	Present observations

Table 4. Light curve characteristics for TYC 2402 0643 1.

Filter	*Phase 0.000*	*Magnitude ± σ* Min. I*	*Phase 0.25*	*Magnitude ± σ* Max. I*
B		–1.302 ± 0.004		–1.776 ± 0.003
V		–0.877 ± 0.002		–1.314 ± 0.005
R		–0.633 ± 0.003		–1.047 ± 0.001
I		–0.399 ± 0.093		–0.752 ± 0.002
Filter	*Phase 0.500*	*Magnitude ± σ* Min. II*	*Phase 0.75*	*Magnitude ± σ* Max. II*
B		–1.375 ± 0.007		–1.756 ± 0.005
V		–0.933 ± 0.008		–1.336 ± 0.007
R		–0.676 ± 0.007		–1.053 ± 0.004
I		–0.399 ± 0.003		–0.754 ± 0.002

Filter	*Min. I – Max. I ± σ*	*Max. I – Max. II ± σ*	*Min. I – Min. II ± σ*
B	0.474 ± 0.010	–0.020 ± 0.018	0.073 ± 0.012
V	0.437 ± 0.013	0.022 ± 0.042	0.056 ± 0.011
R	0.414 ± 0.008	0.006 ± 0.008	0.043 ± 0.010
I	0.353 ± 0.006	0.002 ± 0.002	0.000 ± 0.097

**Magnitude is the variable star – comparison star magnitude.*

Table 5. B, V, R_c, I_c Wilson-Devinney program solution parameters.

Parameters	*Values*
$\lambda_B, \lambda_V, \lambda_R, \lambda_I$ (nm)	440, 550, 640, 790
g_1, g_2	0.32
A_1, A_2	0.5
Inclination (°)	83.40 ± 0.13
T_1, T_2 (K)	5250, 5182 ± 2
Ω	2.2236 ± 0.0011
$q(m_1/m_2)$	0.2079 ± 0.0003
Fill-outs: $F_1 = F_2$ (%)	0.22 ± 0.01
$L_1/(L_1+L_2+L_3)_I$	0.8097 ± 0.0095
$L_1/(L_1+L_2+L_3)_R$	0.8106 ± 0.0083
$L_1/(L_1+L_2+L_3)_V$	0.8124 ± 0.0035
$L_1/(L_1+L_2+L_3)_B$	0.8154 ± 0.0045
JD_o (days)	2457870.51357 ± 0.00006
Period (days)	0. 39943 ± 0.00004
$r_1/a, r_2/a$ (pole)	0.4909 ± 0.0006, 0.2430 ± 0.0011
$r_1/a, r_2/a$ (side)	0.5356 ± 0.0009, 0.2538 ± 0.0013
$r_1/a, r_2/a$ (back)	0.5605 ± 0.0012, 0.2932 ± 0.0026